

Recent results on HH production from ATLAS and CMS

Daniel Guerrero^{a,b,*}

^a*University of Florida,
Gainesville, Florida, United States*

^b*on behalf of the ATLAS and CMS Collaborations*

E-mail: daniel.guerrero@cern.ch

The status and results of the searches for non-resonant and resonant Higgs boson pair production at the LHC are presented. The analyses are performed using partial and full Run-2 proton-proton collision datasets recorded at $\sqrt{s} = 13$ TeV, corresponding to an integrated luminosity of up to about 140 fb^{-1} . The most sensitive results obtained by ATLAS and CMS are reported.

*The Eighth Annual Conference on Large Hadron Collider Physics-LHCP2020
25-30 May, 2020
online*

*Speaker

1. Introduction

The Higgs scalar sector plays a key role in the standard model of particle physics (SM) as it provides a mechanism for the electroweak symmetry breaking (EWSB) and the generation of the mass of vector bosons and fermions. The existence of this sector was proven by the Higgs boson (H) discovery in 2012 by the ATLAS [1] and CMS [2] experiments at the Large Hadron Collider (LHC) [3–5]. Since then, a successful experimental program has measured the Higgs boson properties and its couplings to vector bosons and some fermions [6, 7]. However, the shape of the Higgs energy potential, which determines the Higgs boson self-coupling (λ), remains unmeasured at the LHC. Thus, a measurement of λ is a crucial test of the SM consistency.

In the SM, non-resonant (NR) Higgs boson pair (HH) production gives direct access to λ . In proton-proton (pp) collisions, the dominant production mode is the gluon fusion (ggF) with a cross section at $\sqrt{s} = 13$ TeV of $\sigma_{\text{ggF}}^{\text{SM}}(\text{pp} \rightarrow \text{HH}) = 31.05$ fb evaluated at next-to-next-to-leading order (NNLO) of the perturbative calculation in quantum chromodynamics (QCD) with the resummation at next-to-next-to-leading-logarithm (NNLL) including next-to-leading order (NLO) top quark mass effects [8]. The secondary production mode is the vector boson fusion (VBF) with a cross section at $\sqrt{s} = 13$ TeV of $\sigma_{\text{VBF}}^{\text{SM}}(\text{pp} \rightarrow \text{HHjj}) = 1.73$ fb evaluated at next-to-next-to-next-to-leading order (N³LO) in QCD [9]. The VBF mode gives a unique access to the coupling between a vector boson pair and a Higgs boson pair (VVHH).

Further theoretical considerations (e.g. the hierarchy problem) and experimental observations (e.g. dark matter) suggest the existence of physics beyond the standard model (BSM). BSM models [10–12] that address the shortcomings of the SM predict new spin-0 (X_S) and spin-2 (X_G) resonances decaying with a sizeable branching fraction (\mathcal{B}) to a HH pair. Depending on the model, the mass of the new resonance may vary from 250 GeV to a few TeV. Moreover, the effects of the new states via quantum loops or modification of SM Higgs couplings can induce an enhancement in the NR cross section. The modifiers κ_λ and κ_{2V} quantify the strength of the λ and VVHH couplings with respect to the SM expectation.

This proceeding focuses on the current challenges and strategy towards the experimental quest for HH production at the LHC Run-2 period using a dataset of $\sqrt{s} = 13$ TeV pp collisions with an integrated luminosity (L_{INT}) up to ~ 140 fb⁻¹. Finally, it summarizes the most sensitive direct searches performed by ATLAS and CMS so far.

2. HH experimental quest at the LHC

There is a rich variety of final states to investigate HH depending on the way in which each Higgs boson decays. The current exploration relies largely on the $\text{H} \rightarrow \text{b}\bar{\text{b}}$ decay due to the large $\mathcal{B}(\text{H} \rightarrow \text{b}\bar{\text{b}}) \sim 58\%$, otherwise it becomes statistically limited. Thus far the HH decay channels studied at the LHC are the following: $\text{b}\bar{\text{b}}\text{b}\bar{\text{b}}$ [13–16], $\text{b}\bar{\text{b}}\gamma\gamma$ [17, 18], $\text{b}\bar{\text{b}}\tau^+\tau^-$ [19–22], $\text{b}\bar{\text{b}}\text{VV}$ where V is a W or Z boson [23–28], $\text{W}^+\text{W}^-\text{W}^+\text{W}^-$ [29] and $\gamma\gamma\text{W}^+\text{W}^-$ [30].

The HH signal is reconstructed from objects such as b-quark jets (b), light quark- and gluon-jets (j), tau leptons (τ), muons and electrons (ℓ), photons (γ), and missing transverse energy (MET) from neutrinos (ν). One crucial challenge is the reconstruction of the $\text{H} \rightarrow \text{b}\bar{\text{b}}$ decay, which can be accomplished via two small-radius jets or one large-radius jet depending on the H Lorentz boost. Jet flavour identification is carried out by single-b and double-b taggers based on machine learning (ML) discriminants [31–34]. In addition, an ML-based b-jet energy regression accounts for the energy

mismeasurement caused by neutrinos produced inside the jet or out-of-cone energy leakage [35]. Another key aspect is the reconstruction of the $H \rightarrow \gamma\gamma$ decay. Although the $\mathcal{B}(H \rightarrow \gamma\gamma) \sim 0.2\%$, this decay is reconstructed with $\sim 1\%$ mass resolution.

The current Run-2 analysis strategy uses dedicated techniques such as event categorizations and signal extraction using ML-based discriminants (e.g. boosted decision trees (BDT) and deep neural networks (DNN)). The $\overline{b\overline{b}b\overline{b}}$ final state benefits from $\mathcal{B}(HH \rightarrow \overline{b\overline{b}b\overline{b}}) \sim 34\%$, but suffers from a large amount of QCD multijet background which is modeled using data-driven methods. It is the most sensitive for signals at high m_{HH} values. The $\overline{b\overline{b}}\tau^+\tau^-$ channel is studied in the final states where at least one τ decays hadronically. It is characterized by medium branching fraction and moderate amount of background from top, Z/γ^*+j ets and multijet events. The best channel for low m_{HH} studies is $\overline{b\overline{b}}\gamma\gamma$. Although $\mathcal{B}(HH \rightarrow \overline{b\overline{b}}\gamma\gamma) \sim 0.3\%$, it has a very small background ($\gamma\gamma+j$'s and $H+j$'s) and excellent mass resolution. In addition, the $\overline{b\overline{b}}VV$ holds a good branching fraction but a large top background, and is investigated in VV decays involving j 's, ℓ 's and MET. The $W^+W^-W^+W^-$ channel is explored in multilepton categories. Lastly, the $\gamma\gamma W^+W^-$ channel is studied in WW decays with $2j + \ell + \text{MET}$ final states. Table 1 summarizes the LHC Run-2 analyses.

| | HH channel | Final state and Reference | Signature | $m_{S/G}$ [TeV] | Observable |
|---------------------------------------|-------------------------------------------------------------|----------------------------------------------------------------------------------|------------------|--------------------|-------------------------------------------------|
| ATLAS | $\overline{b\overline{b}b\overline{b}}$ | [13]* | NR [$X_{S/G}$] | [0.26–3.00] | m_{HH} [m_{HH}] |
| | $\overline{b\overline{b}}\gamma\gamma$ | [17]* | NR [X_S] | [0.26–1.00] | $m_{\gamma\gamma}$ [m_{HH}] |
| | $\overline{b\overline{b}}(\tau^+\tau^-, VV)$ | $\tau\tau \rightarrow \tau_{\text{had}}(\tau_{\text{had}}, \tau_\ell)$ [19]* | NR [$X_{S/G}$] | [0.26–1.00] | BDT [BDT] |
| | | $WW \rightarrow \ell\nu 2j$ [27]* | NR [$X_{S/G}$] | [0.50–3.00] | c.e. [m_{HH}] |
| | $\gamma\gamma W^+W^-$ $W^+W^-W^+W^-$ | $WW, ZZ, \tau\tau \rightarrow \ell\nu\ell\nu$ [28]† | NR | - | DNN |
| | | $WW \rightarrow \ell\nu 2j$ [30]* | NR [X_S] | [0.26–0.50] | $m_{\gamma\gamma}$ [$m_{\gamma\gamma}$] |
| | $\ell\nu\ell\nu$ ($\ell\nu\ell\nu, \ell\nu 2j, 4j$) [29]* | NR [X_S] | [0.26–0.50] | c.e. [c.e.] | |
| CMS | $\overline{b\overline{b}b\overline{b}}$ | [14–16]* | NR [$X_{S/G}$] | [0.26–3.00] | BDT [$m_{HH}, m_{HH, \text{red}}$] |
| | $\overline{b\overline{b}}\gamma\gamma$ | [18]* | NR [$X_{S/G}$] | [0.26–0.90] | $m_{\gamma\gamma} \otimes m_{HH}$ |
| | $\overline{b\overline{b}}\tau^+\tau^-$ | $\tau\tau \rightarrow \tau_{\text{had}}(\tau_{\text{had}}, \tau_\ell)$ [21]*[22] | NR [$X_{S/G}$] | [0.25–3.00] | m_{T2} [m_{HH}] |
| | | $WW/ZZ \rightarrow \ell\nu\ell\nu$ [23]* | NR [$X_{S/G}$] | [0.25–0.90] | DNN [DNN] |
| | $\overline{b\overline{b}}(VV)$ | $WW \rightarrow \ell\nu 2j$ [25] | NR [$X_{S/G}$] | [0.80–3.50] | $[m_{\overline{b\overline{b}}} \otimes m_{HH}]$ |
| $ZZ \rightarrow 2\ell(2j, 2\nu)$ [24] | | [$X_{S/G}$] | [0.26–1.00] | [BDT, m_{HH}^T] | |

Table 1: Summary of the ATLAS and CMS searches at the LHC Run-2. The studied signatures are non-resonant (NR), and spin-0 (X_S) and spin-2 (X_G) resonant within the mass range $m_{S/G}$. † indicates full Run-2 data. ★ indicates participation in the partial Run-2 data combination. “c.e.” stands for counting experiment. Note: The full Run-2 results in [20] and [26] are not included here because they were not shown in the talk.

3. Best results with LHC Run-2 data

The most comprehensive and sensitive study of HH production via gluon fusion is carried out by the statistical combination of searches in multiple final states performed by ATLAS and CMS using partial Run-2 data, corresponding to L_{INT} equal to 27.1–36.1 fb^{-1} [36] and 35.9 fb^{-1} [37], respectively. The combined non-resonant and resonant results are summarized as follows.

The sensitivity to search for non-resonant HH production is driven by the $\overline{b\overline{b}b\overline{b}}$, $\overline{b\overline{b}}\gamma\gamma$ and $\overline{b\overline{b}}\tau^+\tau^-$ final states. The study of the κ_λ modifier is obtained by combining information from direct searches marked with a star (★) in Table 1. No statistically significant excess of non-resonant signal events is found across the κ_λ range. For the SM case ($\kappa_\lambda = 1$), upper limits at 95% confidence level (CL) on the signal strength of HH production with respect to the SM expectation correspond to 6.9

(10.0) in ATLAS and 22.5 (12.8) in CMS. The 95% CL observed (expected) allowed interval for the self-coupling modifier is $-5.0 < \kappa_\lambda < 12.0$ ($-5.8 < \kappa_\lambda < 12.0$) in ATLAS, and $-11.8 < \kappa_\lambda < 18.8$ ($-7.1 < \kappa_\lambda < 13.6$) in CMS.

Both ATLAS and CMS searched for new resonances with spin-0 and spin-2 hypotheses in the range of masses from 250 GeV to 3 TeV using multiple final states. The ATLAS and CMS combined results determined that no statistically significant excess of resonant events is observed, and therefore 95% CL upper limits on the production cross section of the new resonances decaying into pairs of Higgs bosons were provided. As an example, the spin-0 combined result in CMS is presented in Figure 1 (left). In addition, the ATLAS combined result included the interpretation of the upper limits as constraints on the parameter space of several BSM models.

The first search for non-resonant and spin-0 resonant production via vector boson fusion is carried out in the $b\bar{b}b\bar{b}$ final state by ATLAS using the full Run-2 dataset [38]. No statistically significant excess of non-resonant and resonant signal events is found across the κ_{2V} parameter range and the mass range 260–1000 GeV, respectively. The non-resonant SM study ($\kappa_{2V} = 1$) yields an observed (expected) limit on the signal strength of HH production via the VBF mode at 950 (550) times the SM prediction. Moreover, as illustrated in Figure 1 (right), the 95% CL observed (expected) allowed interval for the κ_{2V} modifier is $-0.76 < \kappa_{2V} < 2.90$ ($-0.91 < \kappa_{2V} < 3.11$).

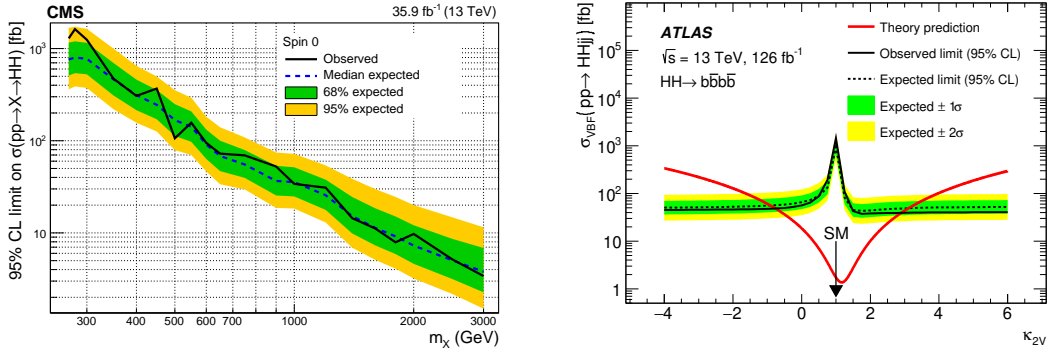


Figure 1: Observed (expected) upper limits at 95% confidence level. Left: Production cross section of a spin-0 resonance decaying to HH as a function of the resonance mass [37]. Right: The non-resonant VBF HH production cross section as function of the κ_{2V} modifier [38].

4. Summary

The exploration of the HH production can shed light on the actual structure of the Higgs boson potential by enabling the study of the Higgs boson self-interaction, and thus giving us a better understanding of the EWSB mechanism. Moreover, it is a unique opportunity to look at new corners of the phase space for new physics in the scalar sector. The study of this signature is stepping up at the LHC and currently involves multiple final states. The development of powerful analysis methods (e.g. ML-based discriminants) are vital to search for this elusive process. Thus far, the current direct searches that explore the ggF and VBF production mechanisms with partial and full Run-2 data do not observe new resonances and anomalous couplings. Hence, upper limits are set on their production cross sections. Moreover, the sensitivity to the SM ggF production cross section is approaching around 10 times the SM prediction. Exciting times are ahead as new full Run-2 results are coming soon and only $\sim 5\%$ of the potential (HL)LHC dataset has been analyzed.

References

- [1] ATLAS Collaboration. The ATLAS Experiment at the CERN Large Hadron Collider. *JINST*, 3:S08003, 2008. doi:[10.1088/1748-0221/3/08/S08003](https://doi.org/10.1088/1748-0221/3/08/S08003).
- [2] CMS Collaboration. The CMS Experiment at the CERN LHC. *JINST*, 3:S08004, 2008. doi:[10.1088/1748-0221/3/08/S08004](https://doi.org/10.1088/1748-0221/3/08/S08004).
- [3] ATLAS Collaboration. Observation of a new particle in the search for the Standard Model Higgs boson with the ATLAS detector at the LHC. *Phys. Lett. B*, 716:1–29, 2012. arXiv:[1207.7214](https://arxiv.org/abs/1207.7214), doi:[10.1016/j.physletb.2012.08.020](https://doi.org/10.1016/j.physletb.2012.08.020).
- [4] CMS Collaboration. Observation of a New Boson at a Mass of 125 GeV with the CMS Experiment at the LHC. *Phys. Lett. B*, 716:30–61, 2012. arXiv:[1207.7235](https://arxiv.org/abs/1207.7235), doi:[10.1016/j.physletb.2012.08.021](https://doi.org/10.1016/j.physletb.2012.08.021).
- [5] CMS Collaboration. Observation of a New Boson at a Mass of 125 GeV with the CMS Experiment at the LHC. *Phys. Lett. B*, 716:30–61, 2012. arXiv:[1207.7235](https://arxiv.org/abs/1207.7235), doi:[10.1016/j.physletb.2012.08.021](https://doi.org/10.1016/j.physletb.2012.08.021).
- [6] ATLAS Collaboration. Combined measurements of Higgs boson production and decay using up to 80 fb^{-1} of proton-proton collision data at $\sqrt{s} = 13 \text{ TeV}$ collected with the ATLAS experiment. *Phys. Rev. D*, 101(1):012002, 2020. arXiv:[1909.02845](https://arxiv.org/abs/1909.02845), doi:[10.1103/PhysRevD.101.012002](https://doi.org/10.1103/PhysRevD.101.012002).
- [7] CMS Collaboration. Combined measurements of Higgs boson couplings in proton-proton collisions at $\sqrt{s} = 13 \text{ TeV}$. *Eur. Phys. J. C*, 79(5):421, 2019. arXiv:[1809.10733](https://arxiv.org/abs/1809.10733), doi:[10.1140/epjc/s10052-019-6909-y](https://doi.org/10.1140/epjc/s10052-019-6909-y).
- [8] M. Grazzini et al. Higgs boson pair production at NNLO with top quark mass effects. *JHEP*, 05:059, 2018. arXiv:[1803.02463](https://arxiv.org/abs/1803.02463), doi:[10.1007/JHEP05\(2018\)059](https://doi.org/10.1007/JHEP05(2018)059).
- [9] F. A. Dreyer and A. Karlberg. Vector-Boson Fusion Higgs Pair Production at N^3LO . *Phys. Rev. D*, 98(11):114016, 2018. arXiv:[1811.07906](https://arxiv.org/abs/1811.07906), doi:[10.1103/PhysRevD.98.114016](https://doi.org/10.1103/PhysRevD.98.114016).
- [10] A. Djouadi et al. The post-Higgs MSSM scenario: Habemus MSSM? *Eur. Phys. J. C*, 73:2650, 2013. arXiv:[1307.5205](https://arxiv.org/abs/1307.5205), doi:[10.1140/epjc/s10052-013-2650-0](https://doi.org/10.1140/epjc/s10052-013-2650-0).
- [11] T. Robens and T. Stefaniak. Status of the Higgs Singlet Extension of the Standard Model after LHC Run 1. *Eur. Phys. J. C*, 75:104, 2015. arXiv:[1501.02234](https://arxiv.org/abs/1501.02234), doi:[10.1140/epjc/s10052-015-3323-y](https://doi.org/10.1140/epjc/s10052-015-3323-y).
- [12] L. Randall and R. Sundrum. A large mass hierarchy from a small extra dimension. *Phys. Rev. Lett.*, 83:3370–3373, 1999. arXiv:[hep-ph/9905221](https://arxiv.org/abs/hep-ph/9905221), doi:[10.1103/PhysRevLett.83.3370](https://doi.org/10.1103/PhysRevLett.83.3370).
- [13] ATLAS Collaboration. Search for pair production of Higgs bosons in the $b\bar{b}b\bar{b}$ final state using proton-proton collisions at $\sqrt{s} = 13 \text{ TeV}$ with the ATLAS detector. *JHEP*, 01:030, 2019. arXiv:[1804.06174](https://arxiv.org/abs/1804.06174), doi:[10.1007/JHEP01\(2019\)030](https://doi.org/10.1007/JHEP01(2019)030).

- [14] CMS Collaboration. Search for nonresonant Higgs boson pair production in the $b\bar{b}b\bar{b}$ final state at $\sqrt{s} = 13$ TeV. *JHEP*, 04:112, 2019. [arXiv:1810.11854](#), [doi:10.1007/JHEP04\(2019\)112](#).
- [15] CMS Collaboration. Search for resonant pair production of Higgs bosons decaying to bottom quark-antiquark pairs in proton-proton collisions at 13 TeV. *JHEP*, 08:152, 2018. [arXiv:1806.03548](#), [doi:10.1007/JHEP08\(2018\)152](#).
- [16] CMS Collaboration. Search for production of Higgs boson pairs in the four b quark final state using large-area jets in proton-proton collisions at $\sqrt{s} = 13$ TeV. *JHEP*, 01:040, 2019. [arXiv:1808.01473](#), [doi:10.1007/JHEP01\(2019\)040](#).
- [17] ATLAS Collaboration. Search for Higgs boson pair production in the $\gamma\gamma b\bar{b}$ final state with 13 TeV pp collision data collected by the ATLAS experiment. *JHEP*, 11:040, 2018. [arXiv:1807.04873](#), [doi:10.1007/JHEP11\(2018\)040](#).
- [18] CMS Collaboration. Search for Higgs boson pair production in the $\gamma\gamma b\bar{b}$ final state in pp collisions at $\sqrt{s} = 13$ TeV. *Phys. Lett. B*, 788:7–36, 2019. [arXiv:1806.00408](#), [doi:10.1016/j.physletb.2018.10.056](#).
- [19] ATLAS Collaboration. Search for resonant and non-resonant Higgs boson pair production in the $b\bar{b}\tau^+\tau^-$ decay channel in pp collisions at $\sqrt{s} = 13$ TeV with the ATLAS detector. *Phys. Rev. Lett.*, 121(19):191801, 2018. [Erratum: *Phys.Rev.Lett.* 122, 089901 (2019)]. [arXiv:1808.00336](#), [doi:10.1103/PhysRevLett.121.191801](#).
- [20] ATLAS Collaboration. Reconstruction and identification of boosted di- τ systems in a search for Higgs boson pairs using 13 TeV proton–proton collision data in ATLAS. 7 2020. [arXiv:2007.14811](#).
- [21] CMS Collaboration. Search for Higgs boson pair production in events with two bottom quarks and two tau leptons in proton–proton collisions at $\sqrt{s} = 13$ TeV. *Phys. Lett. B*, 778:101–127, 2018. [arXiv:1707.02909](#), [doi:10.1016/j.physletb.2018.01.001](#).
- [22] CMS Collaboration. Search for heavy resonances decaying into two Higgs bosons or into a Higgs boson and a W or Z boson in proton-proton collisions at 13 TeV. *JHEP*, 01:051, 2019. [arXiv:1808.01365](#), [doi:10.1007/JHEP01\(2019\)051](#).
- [23] CMS Collaboration. Search for resonant and nonresonant Higgs boson pair production in the $b\bar{b}\ell\nu\ell\nu$ final state in proton-proton collisions at $\sqrt{s} = 13$ TeV. *JHEP*, 01:054, 2018. [arXiv:1708.04188](#), [doi:10.1007/JHEP01\(2018\)054](#).
- [24] CMS Collaboration. Search for the resonant production of a pair of Higgs bosons decaying to the $b\bar{b}ZZ$ final state. CMS Physics Analysis Summary CMS-PAS-HIG-18-013, 2019. URL: <http://cds.cern.ch/record/2682621>.
- [25] CMS Collaboration. Search for resonances decaying to a pair of Higgs bosons in the $b\bar{b}q\bar{q}'\ell\nu$ final state in proton-proton collisions at $\sqrt{s} = 13$ TeV. *JHEP*, 10:125, 2019. [arXiv:1904.04193](#), [doi:10.1007/JHEP10\(2019\)125](#).

- [26] CMS Collaboration. Search for nonresonant Higgs boson pair production in the 4 leptons plus 2 b jets final state in proton-proton collisions at $\sqrt{s} = 13$ TeV. CMS Physics Analysis Summary CMS-PAS-HIG-20-004, 2020. URL: <http://cds.cern.ch/record/2725691>.
- [27] ATLAS Collaboration. Search for Higgs boson pair production in the $b\bar{b}WW^*$ decay mode at $\sqrt{s} = 13$ TeV with the ATLAS detector. *JHEP*, 04:092, 2019. [arXiv:1811.04671](https://arxiv.org/abs/1811.04671), [doi:10.1007/JHEP04\(2019\)092](https://doi.org/10.1007/JHEP04(2019)092).
- [28] ATLAS Collaboration. Search for non-resonant Higgs boson pair production in the $bbl\nu\ell\nu$ final state with the ATLAS detector in pp collisions at $\sqrt{s} = 13$ TeV. *Phys. Lett. B*, 801:135145, 2020. [arXiv:1908.06765](https://arxiv.org/abs/1908.06765), [doi:10.1016/j.physletb.2019.135145](https://doi.org/10.1016/j.physletb.2019.135145).
- [29] ATLAS Collaboration. Search for Higgs boson pair production in the $WW^{(*)}WW^{(*)}$ decay channel using ATLAS data recorded at $\sqrt{s} = 13$ TeV. *JHEP*, 05:124, 2019. [arXiv:1811.11028](https://arxiv.org/abs/1811.11028), [doi:10.1007/JHEP05\(2019\)124](https://doi.org/10.1007/JHEP05(2019)124).
- [30] ATLAS Collaboration. Search for Higgs boson pair production in the $\gamma\gamma WW^*$ channel using pp collision data recorded at $\sqrt{s} = 13$ TeV with the ATLAS detector. *Eur. Phys. J. C*, 78(12):1007, 2018. [arXiv:1807.08567](https://arxiv.org/abs/1807.08567), [doi:10.1140/epjc/s10052-018-6457-x](https://doi.org/10.1140/epjc/s10052-018-6457-x).
- [31] CMS Collaboration. Identification of heavy-flavour jets with the CMS detector in pp collisions at 13 TeV. *JINST*, 13(05):P05011, 2018. [arXiv:1712.07158](https://arxiv.org/abs/1712.07158), [doi:10.1088/1748-0221/13/05/P05011](https://doi.org/10.1088/1748-0221/13/05/P05011).
- [32] CMS Collaboration. Identification of heavy, energetic, hadronically decaying particles using machine-learning techniques. *JINST*, 15(06):P06005, 2020. [arXiv:2004.08262](https://arxiv.org/abs/2004.08262), [doi:10.1088/1748-0221/15/06/P06005](https://doi.org/10.1088/1748-0221/15/06/P06005).
- [33] ATLAS Collaboration. ATLAS b-jet identification performance and efficiency measurement with $t\bar{t}$ events in pp collisions at $\sqrt{s} = 13$ TeV. *Eur. Phys. J. C*, 79(11):970, 2019. [arXiv:1907.05120](https://arxiv.org/abs/1907.05120), [doi:10.1140/epjc/s10052-019-7450-8](https://doi.org/10.1140/epjc/s10052-019-7450-8).
- [34] ATLAS Collaboration. Identification of boosted Higgs bosons decaying into b -quark pairs with the ATLAS detector at 13 TeV. *Eur. Phys. J. C*, 79(10):836, 2019. [arXiv:1906.11005](https://arxiv.org/abs/1906.11005), [doi:10.1140/epjc/s10052-019-7335-x](https://doi.org/10.1140/epjc/s10052-019-7335-x).
- [35] CMS Collaboration. A deep neural network for simultaneous estimation of b jet energy and resolution. 12 2019. [arXiv:1912.06046](https://arxiv.org/abs/1912.06046).
- [36] ATLAS Collaboration. Combination of searches for Higgs boson pairs in pp collisions at $\sqrt{s} = 13$ TeV with the ATLAS detector. *Phys. Lett. B*, 800:135103, 2020. [arXiv:1906.02025](https://arxiv.org/abs/1906.02025), [doi:10.1016/j.physletb.2019.135103](https://doi.org/10.1016/j.physletb.2019.135103).
- [37] CMS Collaboration. Combination of searches for Higgs boson pair production in proton-proton collisions at $\sqrt{s} = 13$ TeV. *Phys. Rev. Lett.*, 122(12):121803, 2019. [arXiv:1811.09689](https://arxiv.org/abs/1811.09689), [doi:10.1103/PhysRevLett.122.121803](https://doi.org/10.1103/PhysRevLett.122.121803).

- [38] ATLAS Collaboration. Search for the $HH \rightarrow b\bar{b}b\bar{b}$ process via vector-boson fusion production using proton-proton collisions at $\sqrt{s} = 13$ TeV with the ATLAS detector. *JHEP*, 07:108, 2020. [arXiv:2001.05178](https://arxiv.org/abs/2001.05178), [doi:10.1007/JHEP07\(2020\)108](https://doi.org/10.1007/JHEP07(2020)108).